Advances in HYDRA and its applications to simulations of Inertial Confinement Fusion Targets

M. M. Marinak, G. D. Kerbel, J. M. Koning, M. V. Patel,
S. M. Sepke, B. Chang, P. Michel, D. Larson

Lawrence Livermore National Laboratory

22nd International Conference on the Numerical Simulation of Plasmas
Long Branch, New Jersey

September 7-9, 2011

LLNL-PRES-496758

This work was performed under the auspices of the U.S. Department of Energy by Lawrence Livermore National Security, LLC, Lawrence Livermore National Laboratory under Contract DE-AC52-07NA27344

Outline

New features enable the HYDRA 2D/3D ICF code to simulate a broader range physical effects

We apply several new capabilities to problems of interest

- Monte Carlo neutron, gamma ray and charged particle transport
  - Enables simulations of the effects of various asymmetries and their signature on neutron diagnostics
- Polar S_N multigroup radiation transport package
  - Enables 2D simulations of instability growth seeded by features on NIF capsules to achieve greater accuracy
- Inline model for energy transfer between crossed laser beams
  - Enables self-consistent treatment
- Detailed Configuration Accounting (DCA) model enables more accurate treatment of NLTE kinetics
- Fast electron transport code Zuma integrated with HYDRA
  - Integrated simulations of fast ignition targets
  - HYDRA's Inline 3D MHD package used to study implosions with pre-imposed fields

HYDRA is a 2D/3D multiphysics ICF simulation code that is applied by users at various institutions to simulate a wide variety of ICF/High Energy Density Targets

- Development of HYDRA is a collaborative effort between LLNL and SNL
- HYDRA is used at SNL, Rochester LLE, LANL, LBNL and various universities (10 external institutions)
- HYDRA is applied to a wide variety of targets including:
  - Indirect drive capsules only simulations of NIF, Omega, Nova experiments
  - Direct drive capsule only simulations
  - Integrated hohlraum simulations (ignition, symcaps, re-emission, shock timing)
  - Heavy ion ignition target designs, Warm Dense Matter experiments
  - Z-pinches
  - Theta pinch (Xe studies for LIFE)
  - Fast ignition integrated target design
  - Planar Rayleigh-Taylor targets
  - Direct drive jet formation experiments
  - …

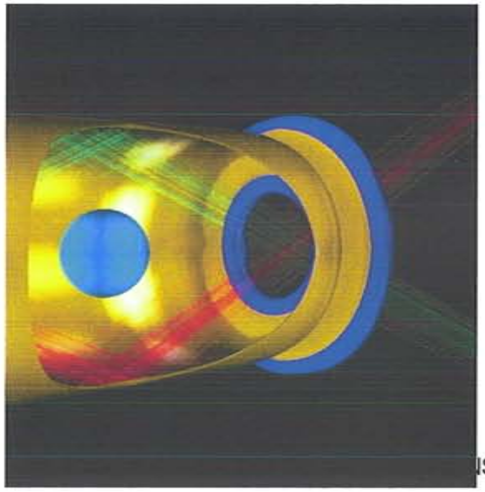

Physical processes modeled by the HYDRA code for ICF simulations

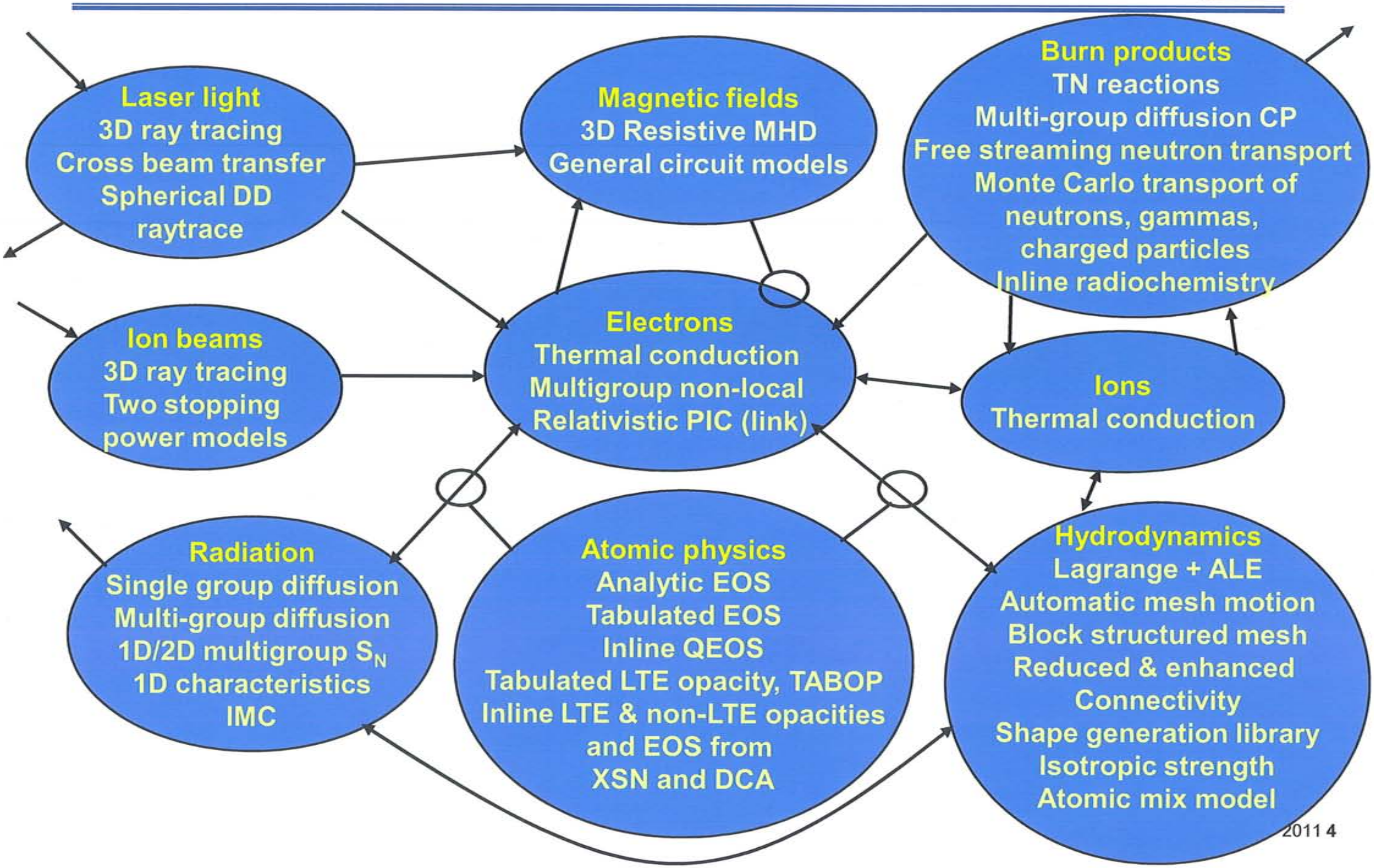

A Monte Carlo transport package for neutrons, gamma rays and charged particles is installed

- **We have incorporated the LLNL Arrakis code into HYDRA to perform Monte Carlo calculation of burn product transport**
- **In flight reactions are treated**
- **Arakkis is a parallel scaleable library with dynamic load balancing capability**
- **Includes expanded set of thermonuclear reactions, such as T-T -> 2n + α three body reaction**
- **Temperature and fluid motion effects are modeled**
- **Models the full set of NIF particle diagnostics such as Neutron Time of Flight, Magnetic Recoil (MRS), Gamma Ray Histories (GRH) and neutron imaging**

NIF Diagnostics

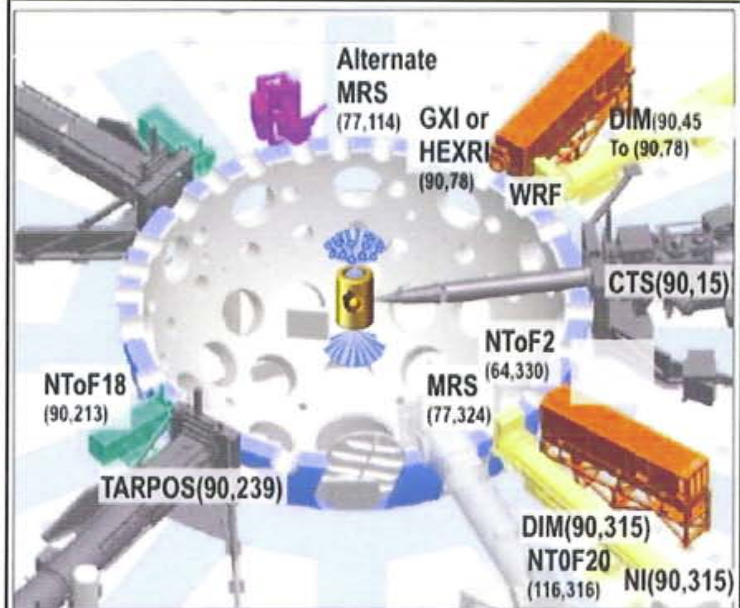

HYDRA can now model the full set of NIF particle diagnostics

We examine the neutron signature of a NIF ignition capsule implosion having a large P1 thickness variation

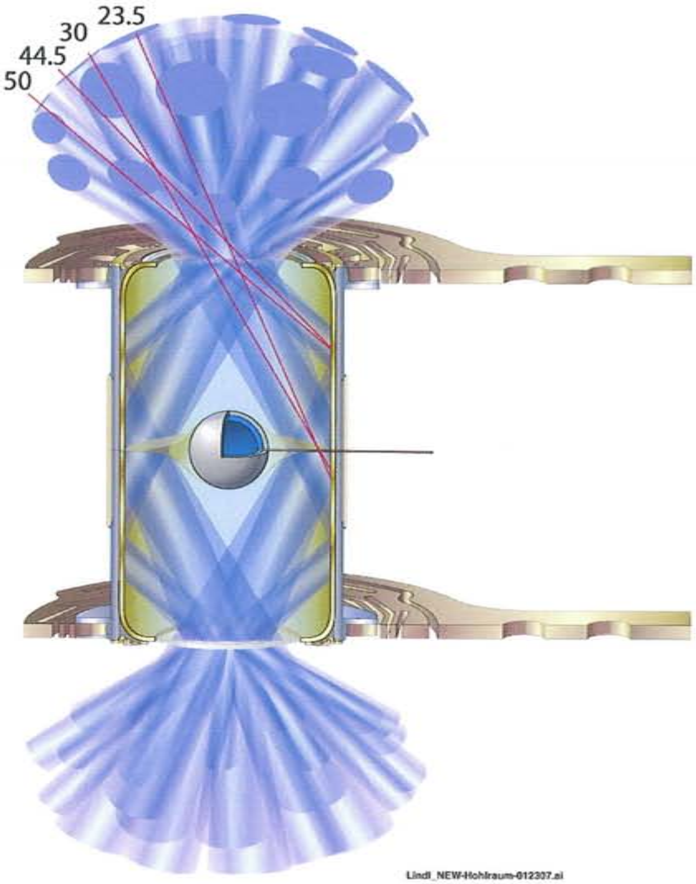

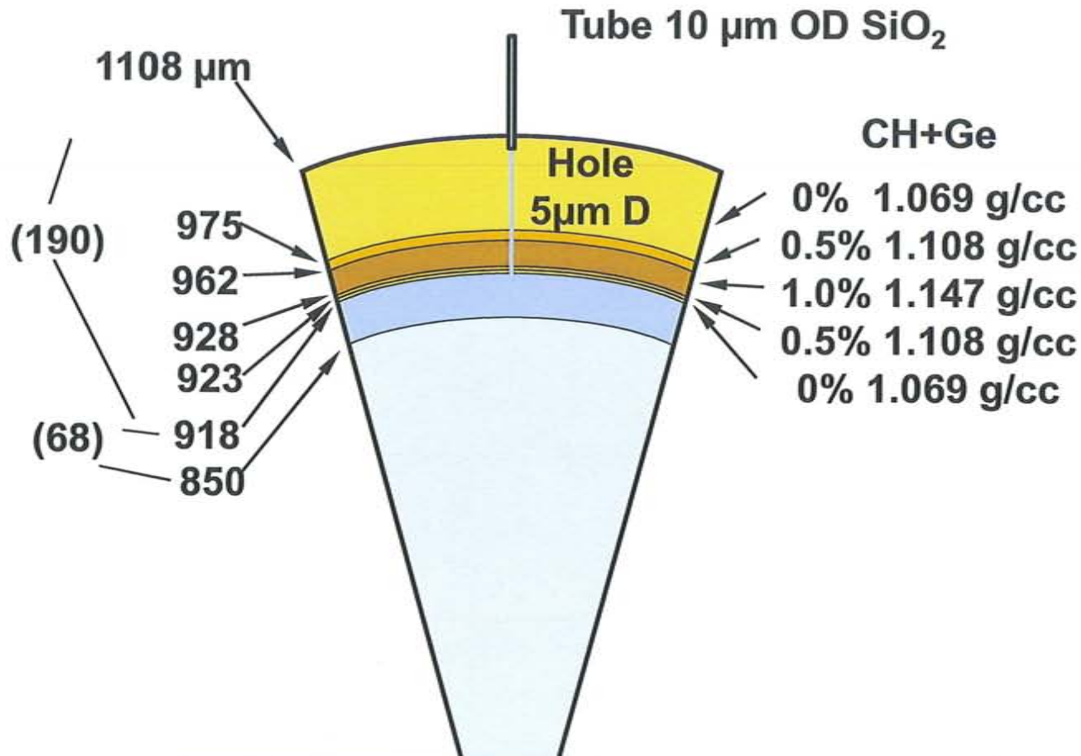

Fuel	ρ	D at%	T	^1H
Solid	0.255 g/cc	6	72	22
Gas	0.3 mg/cc	0.7	7.3	92

Surface roughness includes a 2 micron peak to valley thickness variation in ablator
Neutron diagnostics are primarily sensitive to low mode asymmetries with ℓ <= 3

Full capsule only simulation (4π) includes intrinsic drive asymmetry and severe surface roughness

Intrinsic drive asymmetry obtained from 3D HYDRA integrated hohlraum simulation

Simulation includes roughnesses on ice and ablator surfaces through intermediate modes (ℓ <= 120), including 2 μm peak-to-valley P1

Roughness initialized on inner ice surface taken from NIF specification scaled by 0.5

Roughness initialized on ablator in range $\ell > 10$ were 60 nm rms, ~ 8x NIF specification

Ablator surface roughness spectra

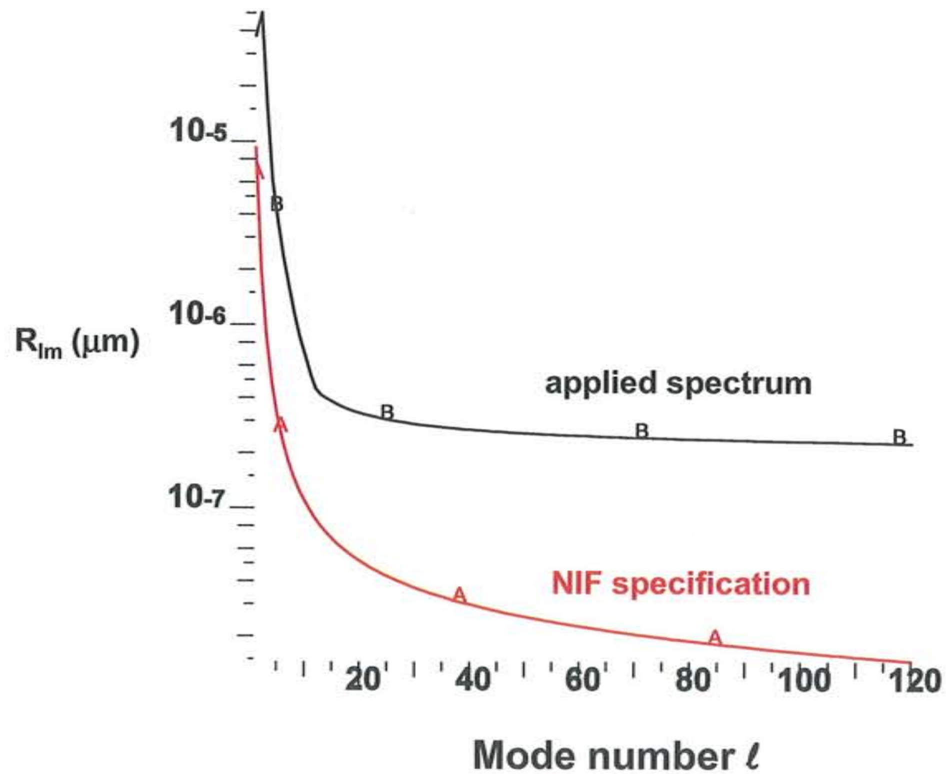

Severe perturbation applied in intermediate modes on ablator

Ablator bubbles penetrate shell before peak implosion velocity is obtained

Full 3D capsule simulation transporting neutrons, charged particles and gamma rays

57.9 million zones run on 4096 processors

Surface roughness modes initialized using full set of spherical harmonics through $\ell = 120$

115 million particles transported at peak

Cut away view of density 2.0 g/cm³ contour in capsule shell at 20.18 ns

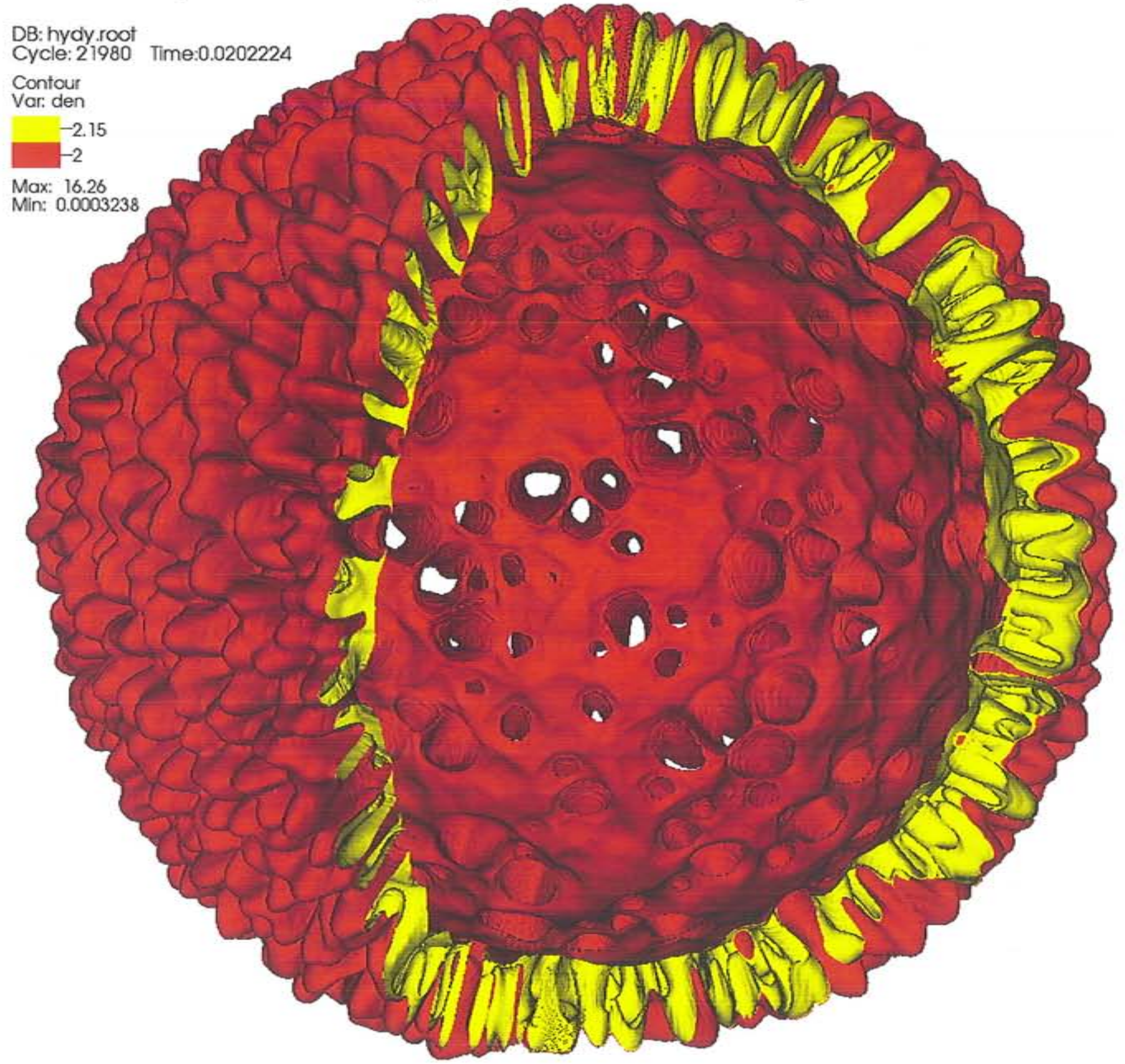

Hot spot assembly strongly perturbed by high mode RT compromising shell during implosion phase

Density contours (g/cm^3)

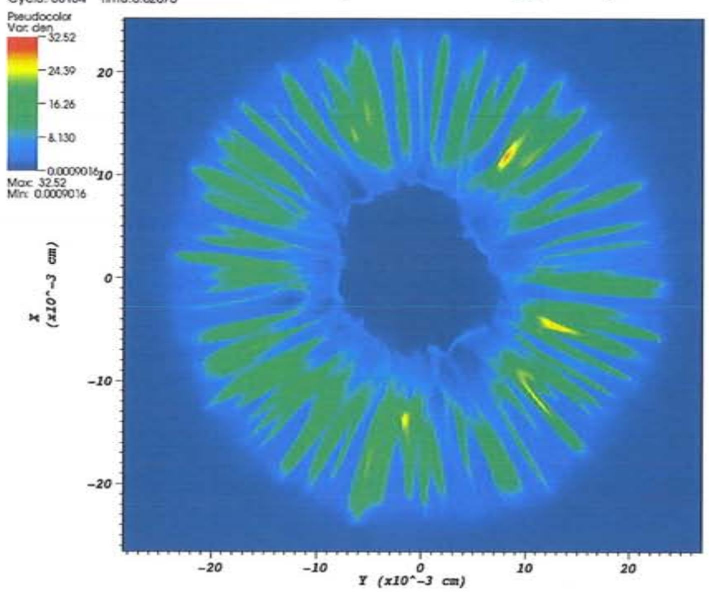

Material boundaries

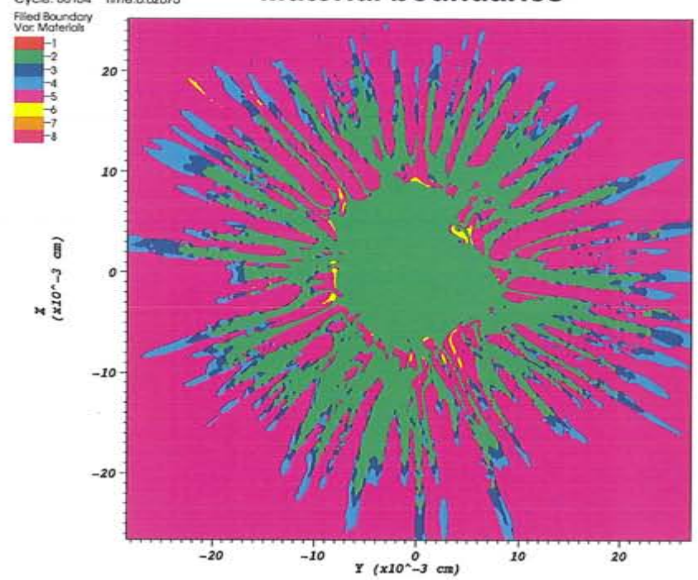

Contours in equatorial plane at 20.75 ns
310 psec before bang time

Primary neutron yield 1.26x10^{14}
Energy yield 353 J

Downscattered neutron fraction average 0.0272 average range 0.02 – 0.034

Burn weighted ion temperature 1.22 keV

Ion temperature (keV)

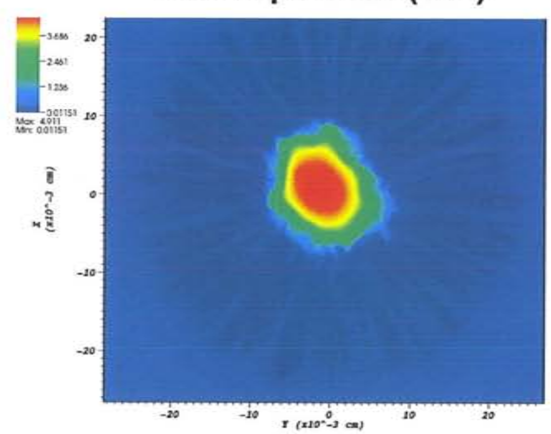

Various neutron diagnostics clearly show P1 asymmetry even with severe mix

Neutrons clearly show hot spot velocity is Doppler shifted by 30 km/s
Direction of Doppler shift correlates with orientation of P1 initial ablator thickness variation

P1 also visible in downscattered fraction

Large spectral shape distortion relative to a Gaussian (w=0.84). Indicates burn occurred over unusually broad range of temperatures.

FWHM burn temperature directional variation 1.08 to 1.40 keV (7 parameter fit) indicating significant non-spherical velocity (ℓ=2)

P1 asymmetry would be detectable with ~12 detectors scattered around solid angle measuring primary yield as long as relative measurement accuracy good to (+/- 3 %)

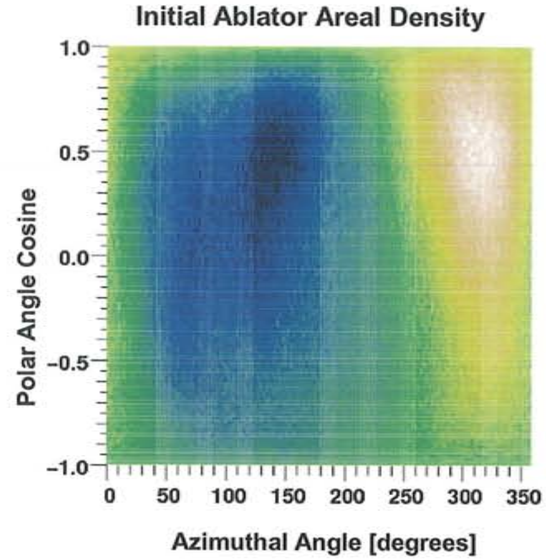

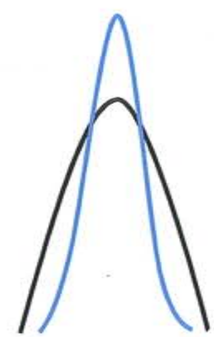

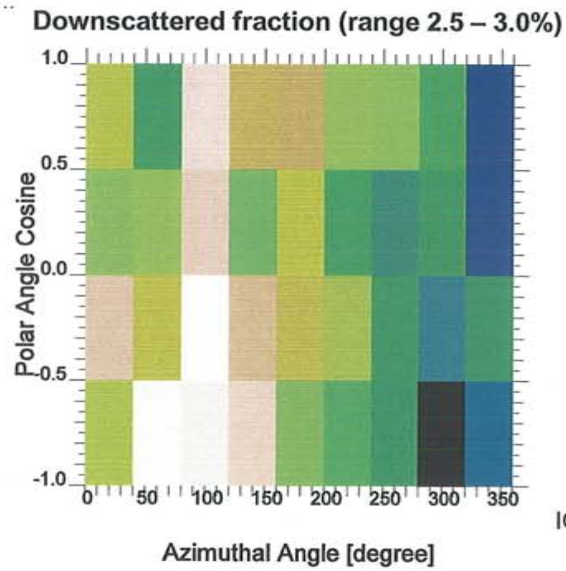

A new polar S_N deterministic method for radiation transport is available in HYDRA

- Polar S_N converges with second order accuracy without significant ray effects
- Should enable more accurate treatment of fill tube calculations, radiation transport in hohlraums
- Development in collaboration with CASC (Center for Applied Scientific Computing)
- Presently runs on meshes of orthogonal quadrilaterals (2D)

Polar Sn offers higher accuracy through its novel formulation for discretizing the transport equation along a ray

$$\frac{d\psi}{ds} = q - \sigma\psi + \int_{S^2} \sigma(\vec{\Omega}\cdot\vec{\Omega}')\psi d\vec{\Omega}'$$

Polar S_N maintains exact spherical symmetry in test problems

Capsule with fill tube provides stringent test of polar S_N transport method's convergence

- Consider the shadow initially cast by a 12.5 μm diameter fill tube on baseline plastic ignition target design
- Fill tube initially covers just 0.00072% of capsule surface
- The tube's extremely small diameter and discontinuous opacity jump at the start provide the most challenging conditions to calculate

Initial material boundaries

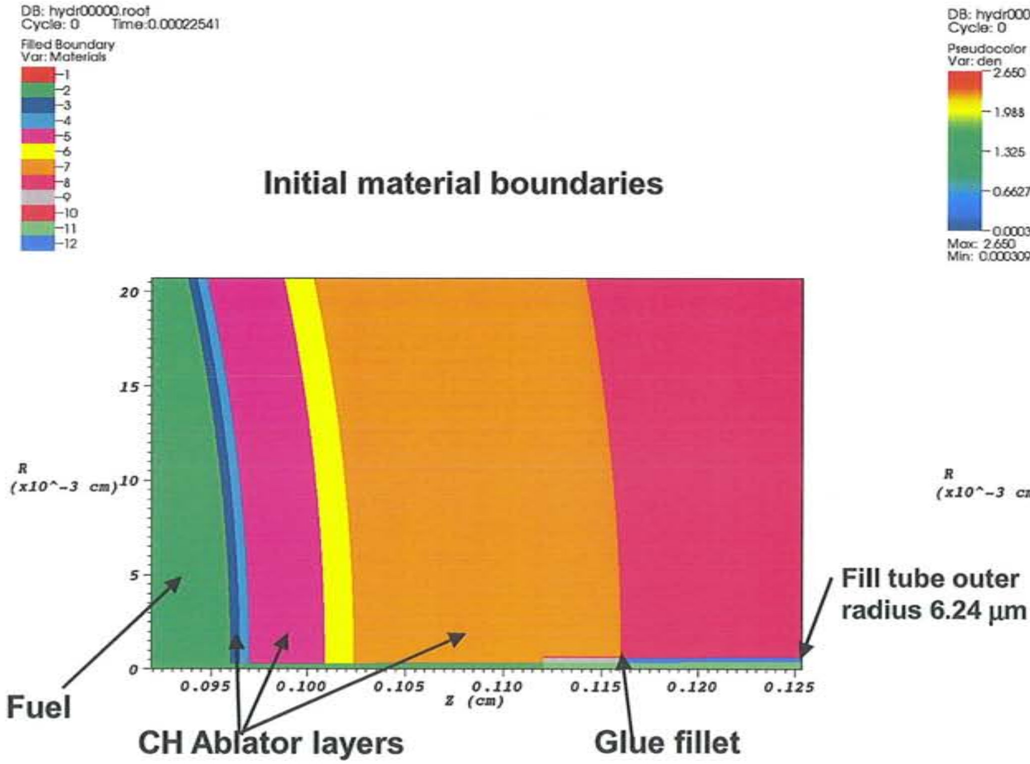

Initial density [g/cm³]

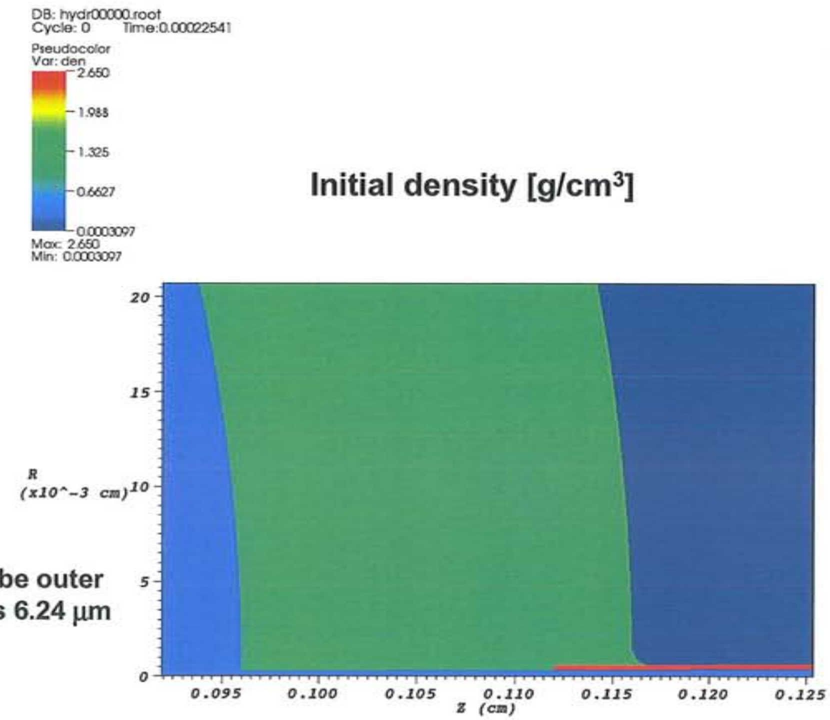

Radiation energy density on capsule surface agrees well with analytic solution for fill tube problem

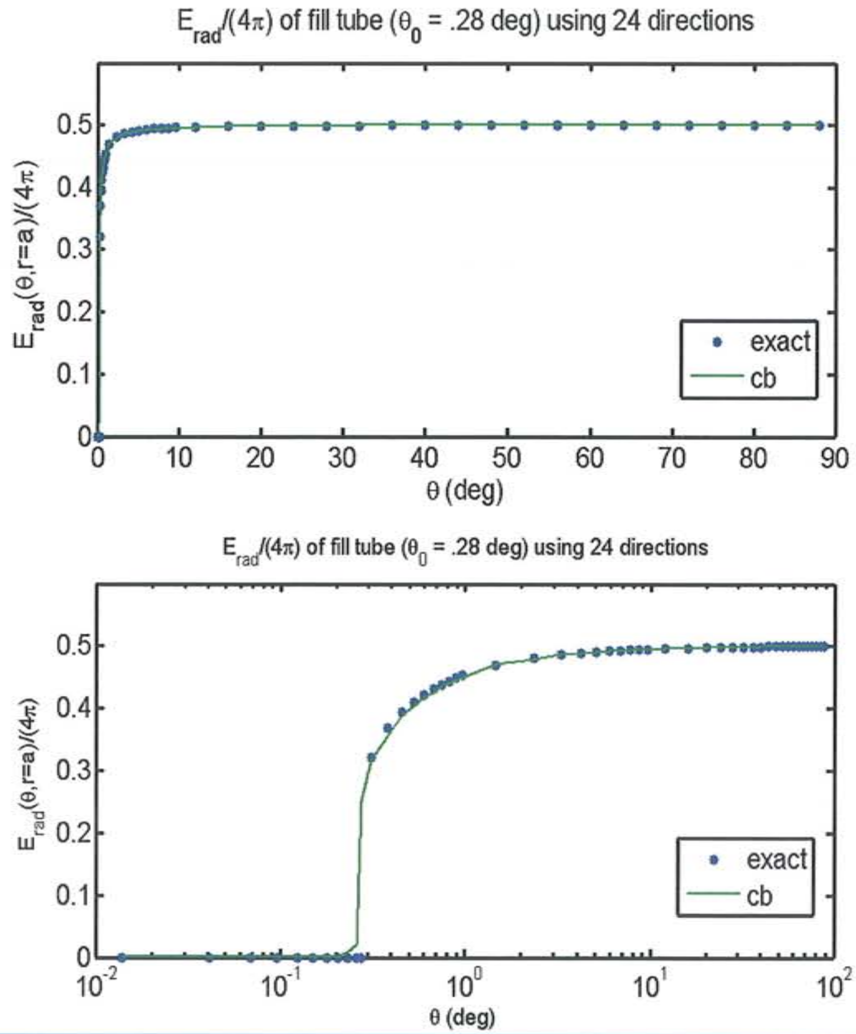

Used 6 azimuthal and 4 polar ray directions

Extent of fill tube shadow correctly modelled using 24 ray directions

Comparison of implosion simulations of NIF capsule with fill tube show excellent correspondence in weakly nonlinear phase

Density Profiles at 17.66 ns

Multigroup Diffusion

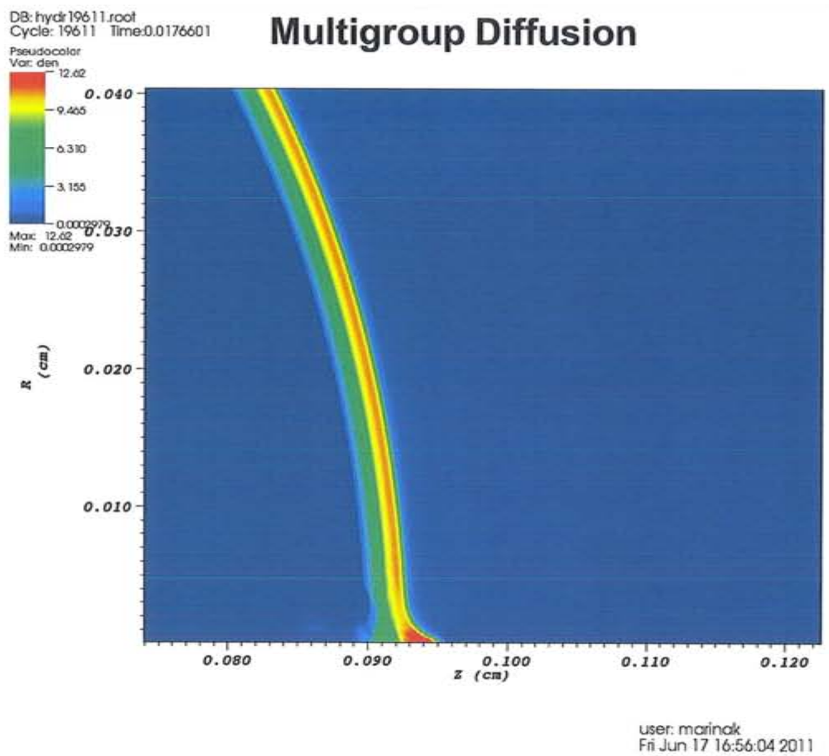

Polar S_N

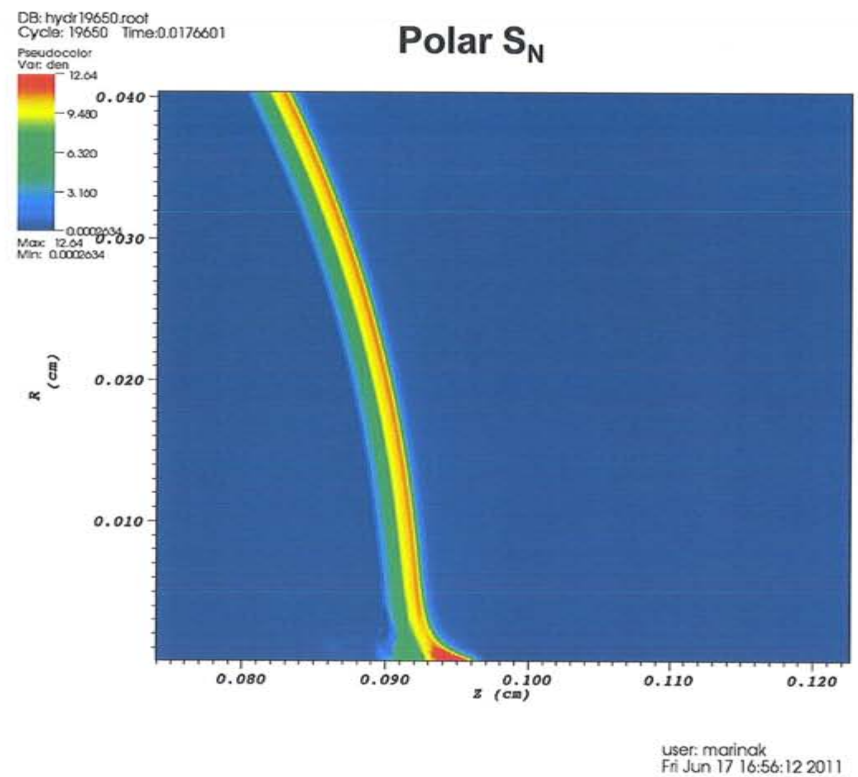

Calculations run with 60 energy groups
Polar S_N run with 24 angles
Simulation domain is half a quadrant

Highly nonlinear perturbation generated by spike eventually attains larger amplitude with polar S_N transport

Density profiles at 20.6 ns

Multigroup Diffusion

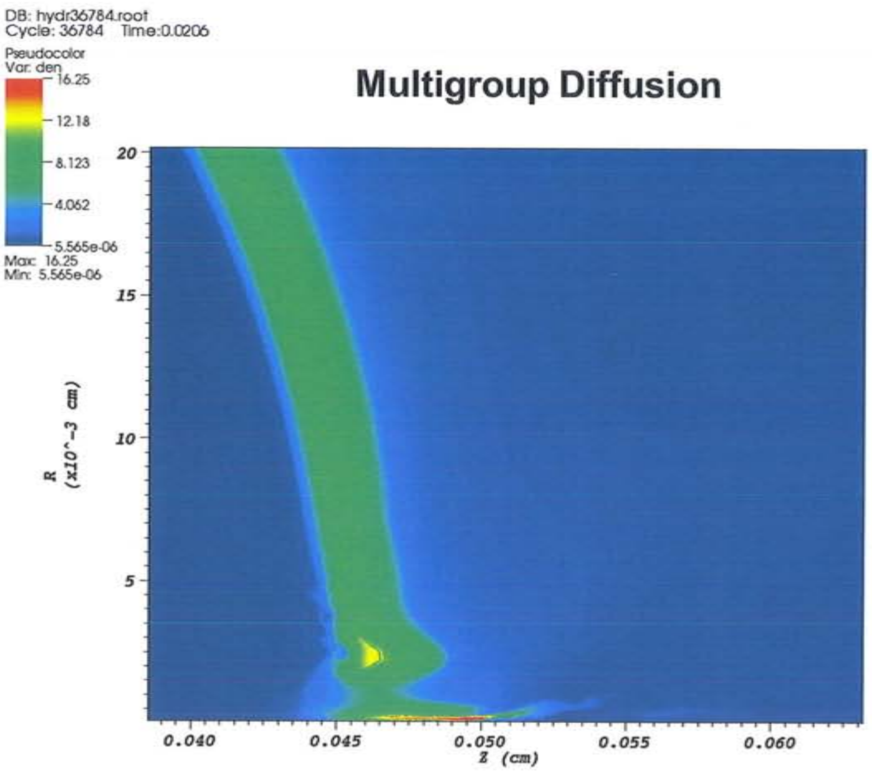

Polar S_N

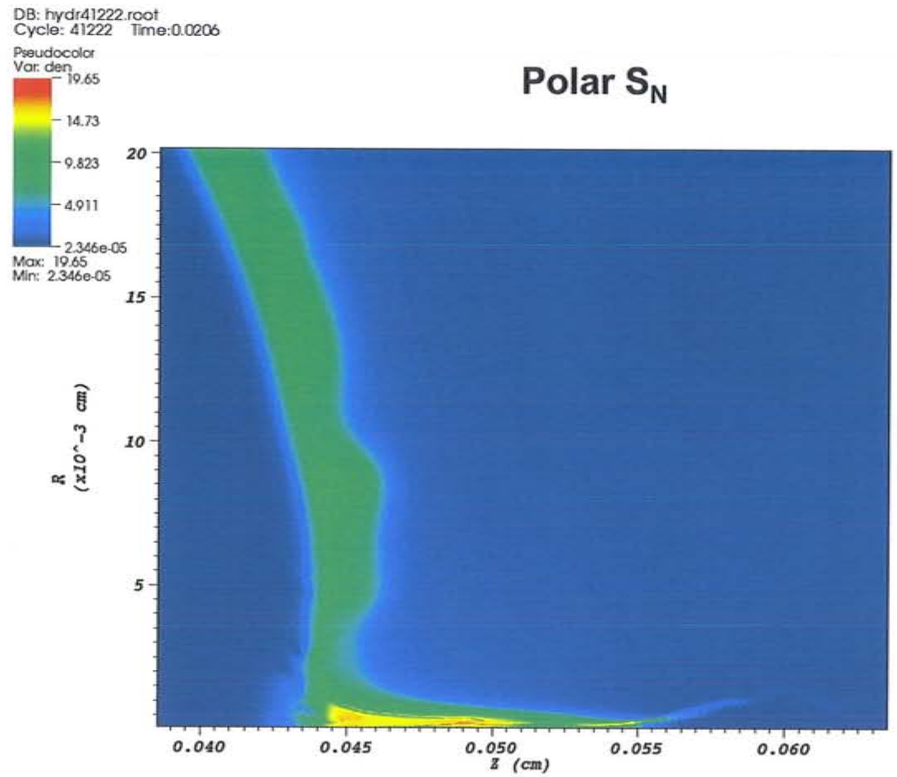

Larger amplitude is consistent with effect of self-shielding
This is treated more accurately with polar S_N

Energy transfer between crossed laser beams can now be treated with an inline model in HYDRA

- **Energy transfer occurs when the beat frequency between crossed laser beam nearly satisfies the resonance condition**

$$\omega_0 - \omega_1 = \left|k_0 - k_1\right| c_s + \left(k_0 - k_1\right) \cdot V$$

- **We have implemented a linear model[1] for energy transfer in HYDRA's 3D laser raytracing package**
- **Cross beam energy transfer equations can be written in the form**

$$\frac{\partial}{\partial \tau_1} I_1 = C_{12} I_1 I_2$$

$$\frac{\partial}{\partial \tau_2} I_2 = C_{21} I_1 I_2$$

- **Coupling coefficients C_{12}, C_{21} require evaluations of the electron and ion susceptibilities χ_e, χ_i with respect to beat ion accoustic wave**

1. P. Michel et. Al, Phys. Plasmas **17**, 056305 (2010)

Inline cross beam energy transfer model produces self-consistent result

- Solution to ray equations must be iterated since the coupling rate depends upon beam intensities
- Zonal intensities are recalculated during each iteration by accumulating the contributions for each ray in each beam, including cross beam coupling
- Excellent energy conservation obtained
- An empirical saturation model limits the allowed density fluctuations in the ion accoustic beat waves
- Model produces self-consistent treatment of cross beam transfer
- Runs either on general 3D or axisymmetric 2D meshes

3D simulation of reemission sphere with inline model produces results close to those obtained with post-processed technique

Integral (P2)_vs_time/Integral(P0)_at final_time

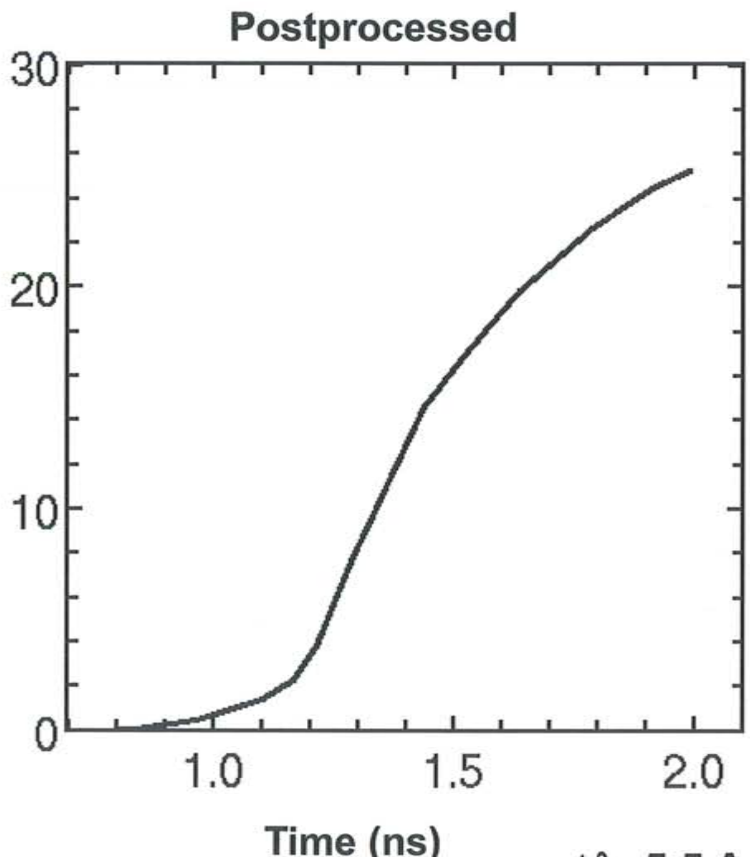

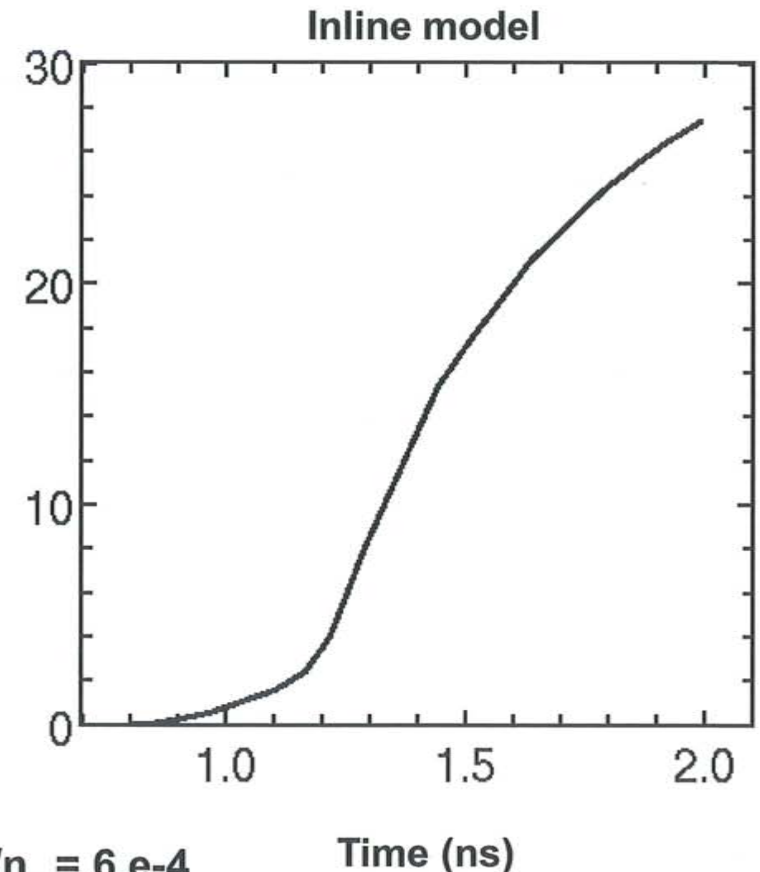

$\Delta\lambda$=5.5 A and $\Delta n_e/n_e$ = 6.e-4

NIF Hohlraum simulations also benefit from more accurate models for NLTE opacities obtained from DCA and from a model for non-local electron transport

Simulations of fast ignition

HYDRA performs integrated simulations of fast ignition designs. This indirectly driven cryogenic capsule is mounted on a gold cone.

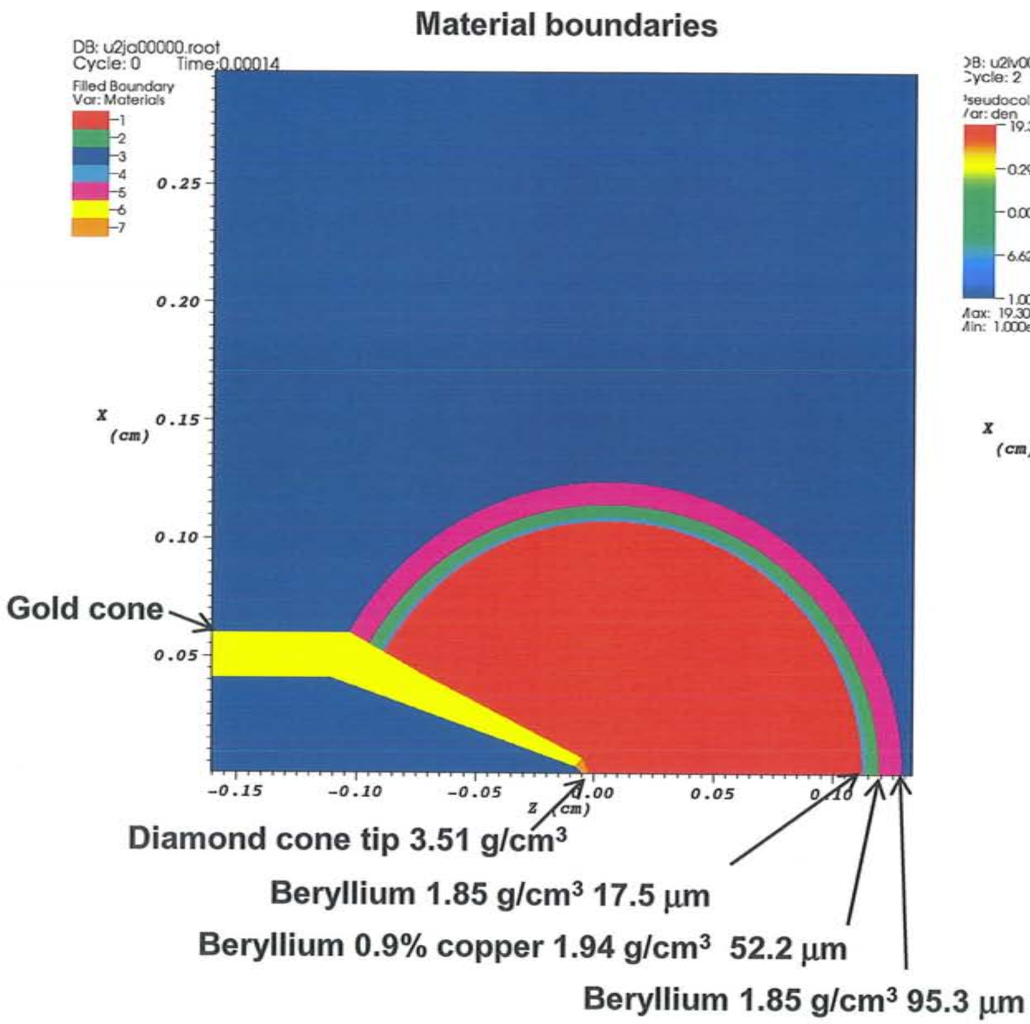

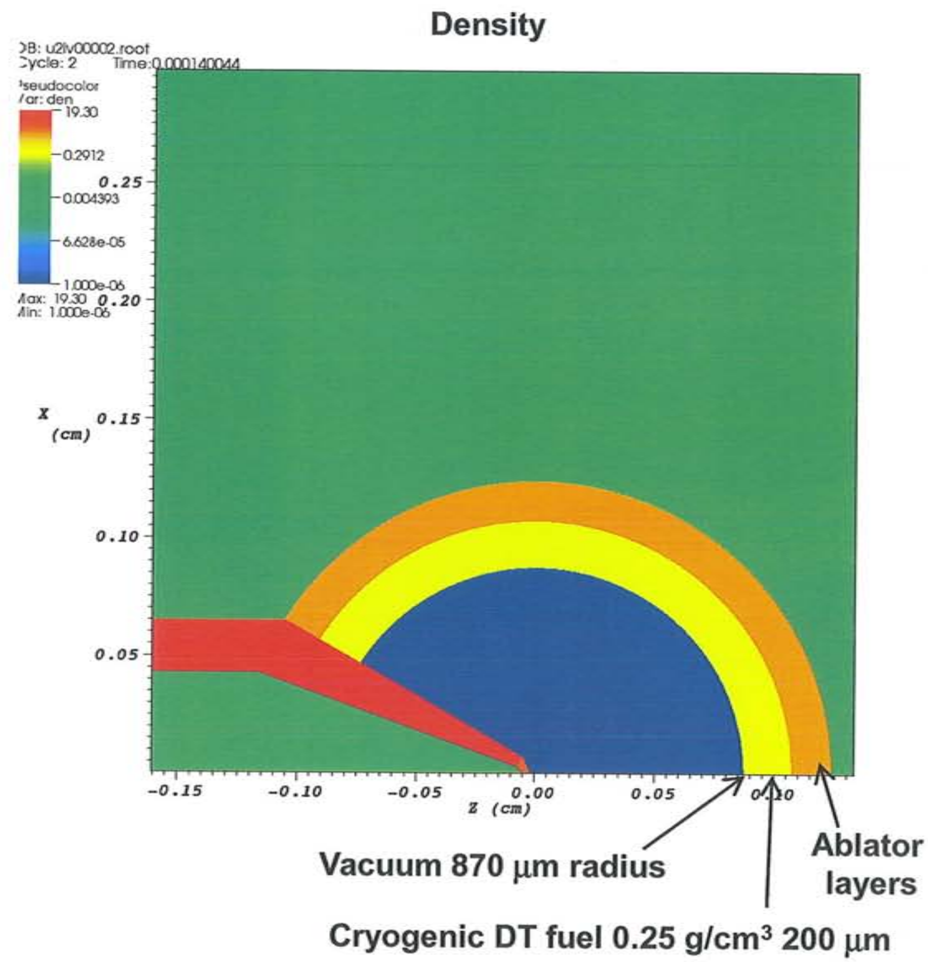

Planckian x-ray drive spectrum uses temperature obtained from 1-D hohlraum simulation producing single shock drive. Hohlraum driven by 570 kJ NIF-like laser pulse lasting 32 ns.

One design has a preimposed axial magnetic field to guide fast electrons to the dense fuel

Initial axial field

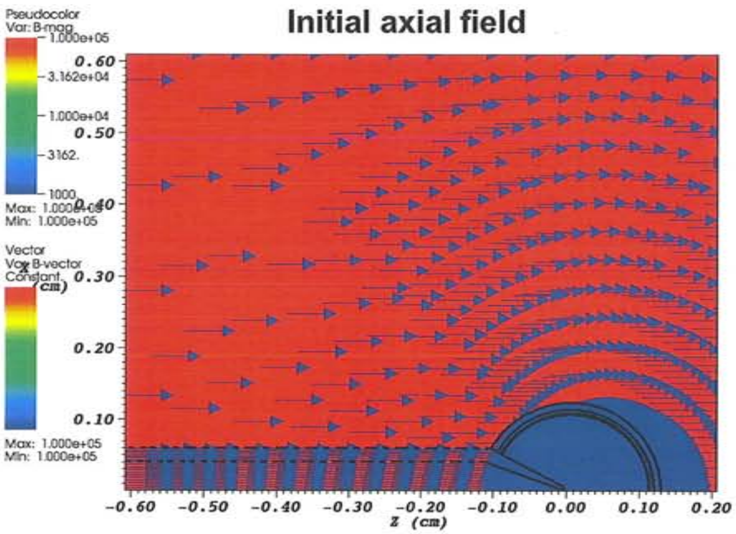

Pseudo-color in log B
Contours for DT ρ at ignition time

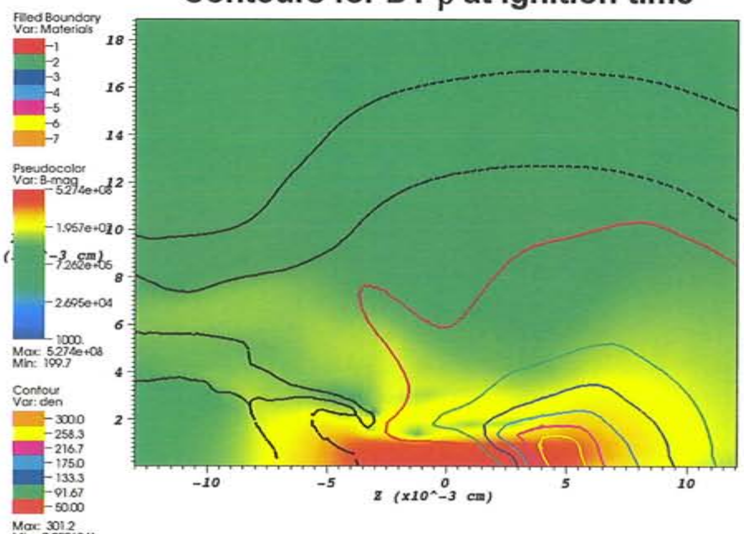

Initial conditions: uniform Bz = 100kG

Pseudo color in log B at 32 ns

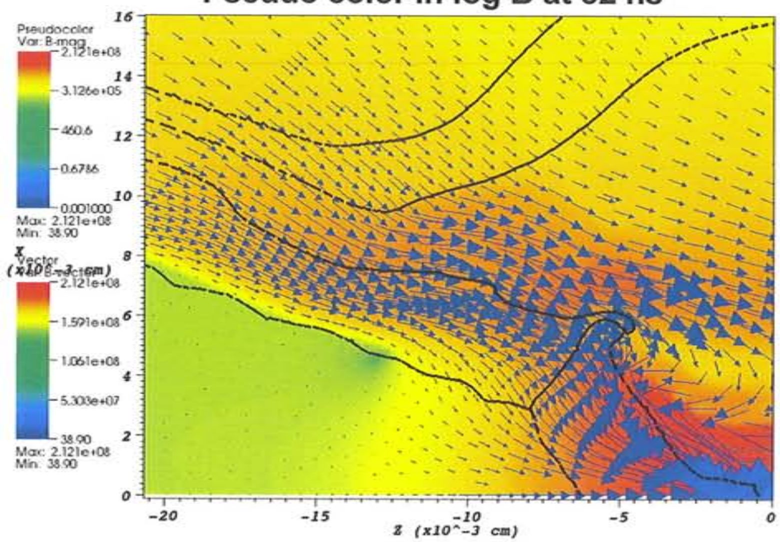

- **Preimposed magnetic field is compressed by capsule implosion yielding over 500 MG near axis**
- **Simulation utilizes HYDRA's 3D MHD package**
- **Hot electrons created in cone tip must overcome magnetic mirroring**

HYDRA is linked to Zuma to perform 2D/3D integrated hydrodynamics/burn simulations including transport of electrons from ultra high intensity short pulse lasers

- Zuma, is a relativistic particle in cell code for modelling transport of relativistic electrons in dense plasmas
- Zuma models the background high density plasma as a resistive fluid while the fast electrons are treated kinetically
- HYDRA plasma profiles are linked to Zuma
- After advancing a suitable time the energy deposition rate, momentum deposition rate and magnetic field are linked to HYDRA
- HYDRA advances to same time as Zuma and process repeats for a self-consistent simulation

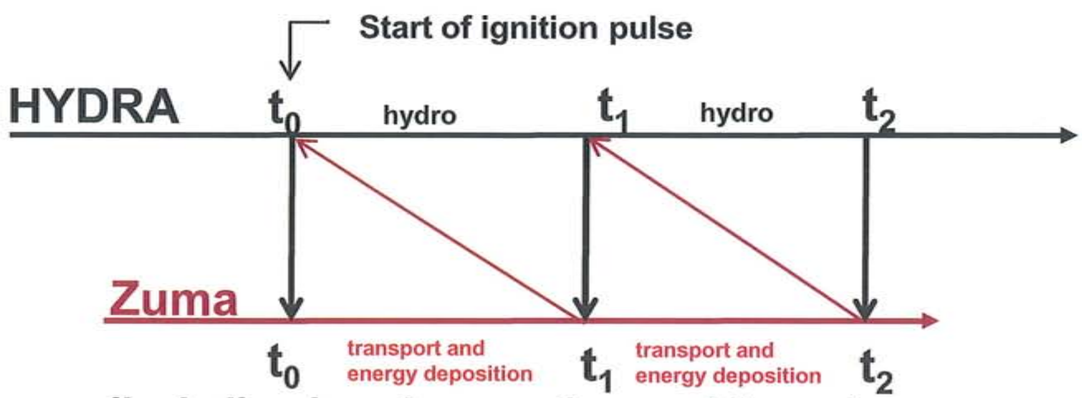

Two codes can use dissimilar domains, meshes and time steps

Data exchange and codes managed automatically by a control script written in Yorick[1]

1. See http://yorick.sourceforge.net

Isochoric high density fuel designed to assemble at a distance from cone tip to maintain cone integrity

Time of peak compression – 32.4 ns

Density

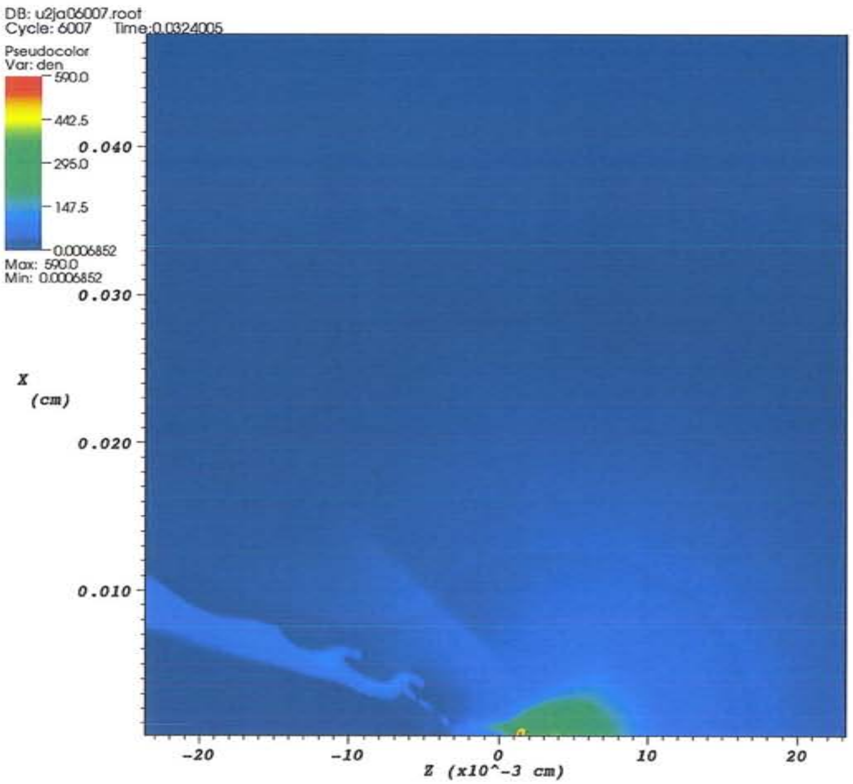

Material boundaries

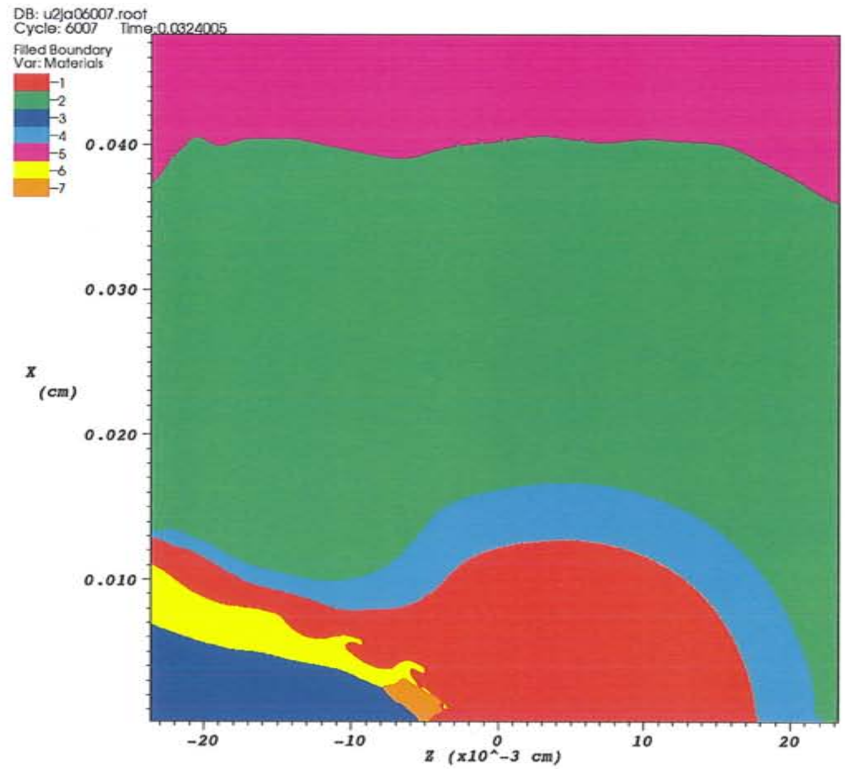

Compressed fuel diameter of ~ 100 μm

Conflicting demands of bringing cone tip close to dense fuel and reducing pressure on cone tip represent a principal design challenge

At peak compression electron source launched from cone

- For this calculation short pulse laser has 10 psec pulse duration

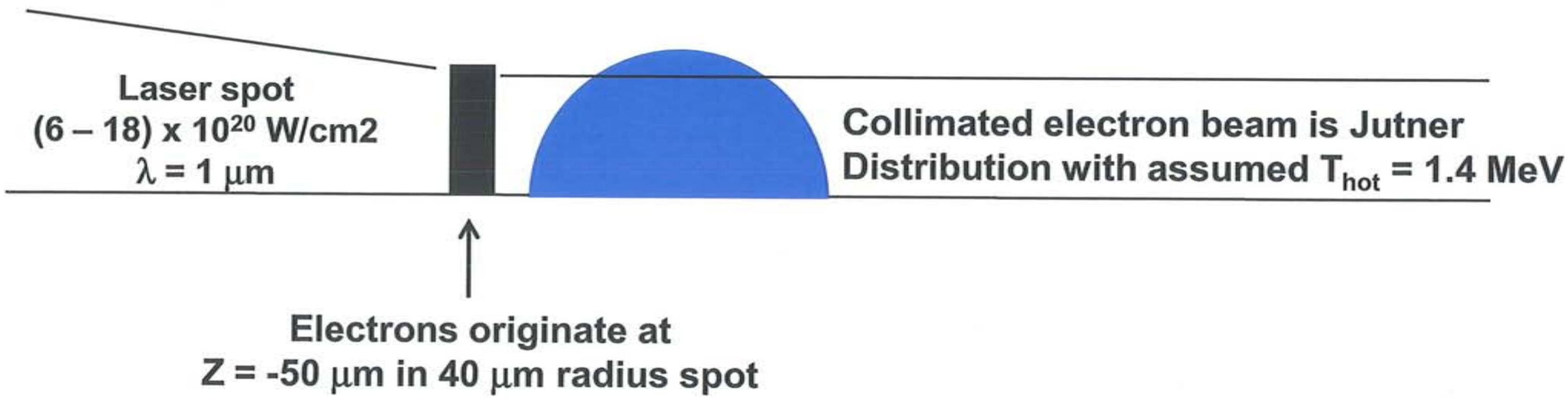

Electron beam in full 3D simulation develops filamentary structure

10 psec into electron pulse

Contours of e⁻ energy deposition rate

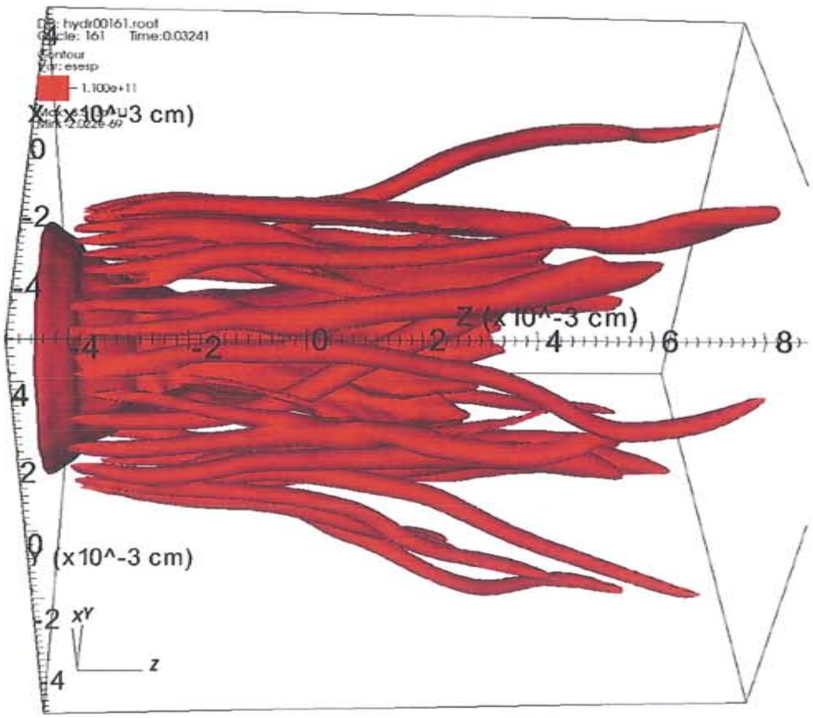

Electron energy deposition rate (EU/cm/μsec)

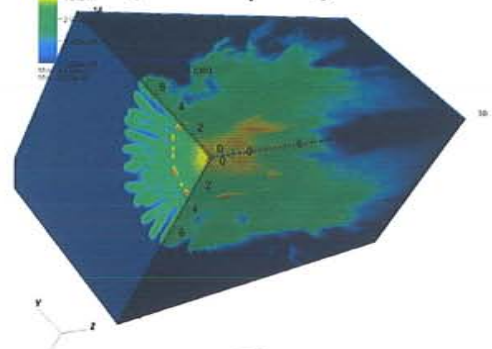

z = -20 μm

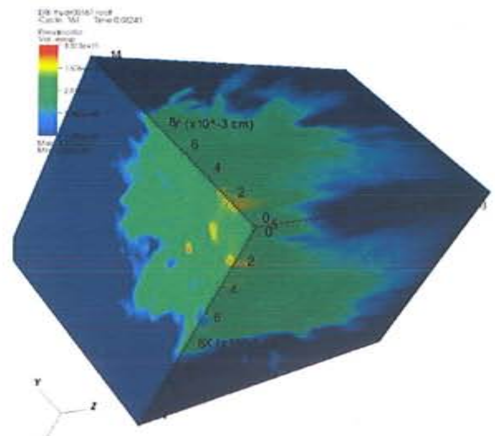

z = +50 μm

Cut planes at x = 0, y = 0

3D simulation initialized with axisymmetric profiles at beginning of electron pulse
47.7 million zones in HYDRA mesh with 100 million IMC photons run on 1024 processors
36 million zones in Zuma mesh - 1 μm resolution on each mesh

Electron beam range is increased in filaments due to local density troughs

Density (g/cm³)

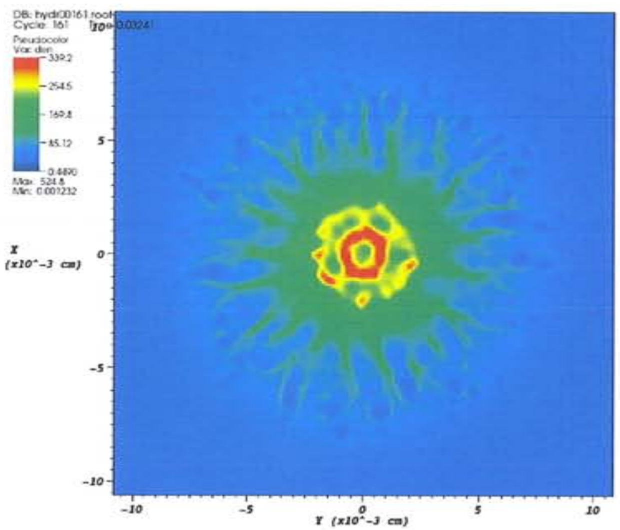

Te (KeV)

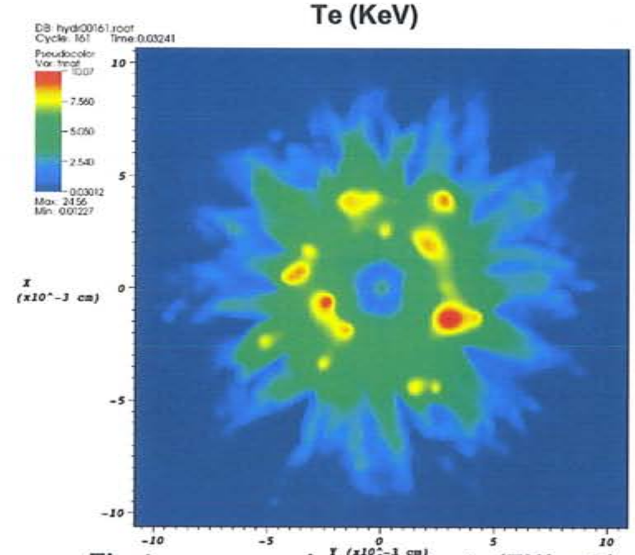

Electron energy deposition rate (EU/cm3/μsec)

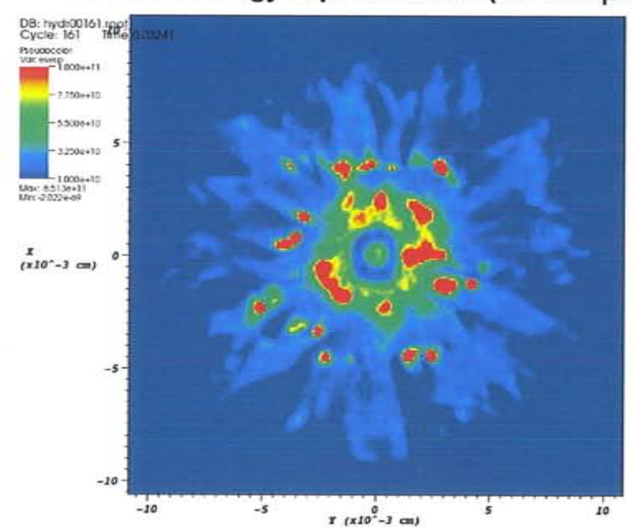

Profiles at z= +50 μm at 10 psec into electron pulse

Concentrated electron heating within beam filament results in reduced density there as local pressure profile relaxes

This results in lower minimum densities in 3D, resulting in longer range for electrons

Results in higher escaped electron energy

New features enable the HYDRA 2D/3D ICF code to simulate a broader range physical effects

We applied several new capabilities to problems of interest

- First high resolution 3D simulation of full NIF capsule sphere included Monte Carlo neutron, gamma ray and charged particle transport
  - Provided diagnostic signatures for low mode asymmetry in presence of severe mix
  - Provides guidance on requirements for diagnostics to measure effects
- Polar S_N multigroup radiation transport package
  - High resolution 2D simulation of instability growth seeded by a fill tube on a NIF capsule showed larger perturbation growth in nonlinear regime
- Inline model for energy transfer between crossed laser beams
  - Enables self-consistent treatment
- Detailed Configuration Accounting (DCA) model enables more accurate treatment of NLTE kinetics
- Fast electron transport code Zuma integrated with HYDRA
  - 3D integrated simulation of fast ignition target showed increased range of fast electrons due to beam filamentation
  - HYDRA's inline 3D MHD package used to study implosions with pre-imposed fields

- END

- Supplementary viewgraphs follow

Zuma: code description

- Zuma is a three-dimensional hybrid plasma simulation code for modeling the transport of relativistic electrons in dense plasmas. The background high density plasma is modeled as a resistive fluid while the fast electrons are treated kinetically.
- These assumptions are appropriate for high density, relatively cool, quasi-neutral plasmas where kinetic effects are strongly damped by the plasma collisionality[1,2].
- The kinetic fast electrons are slowed by interaction with the background electrons and scatter off both the background ions and electrons. This process is modeled via the drag and scattering formulas reported by Atzeni, Schiavi and Davies[3].
- Zuma can run in 2D or 3D Cartesian geometry or 2D axisymmetric geometry

- [1] J. R. Davies, *Phys. Rev. E*, 65, 026407 (2002).
- [2] L. Gremillet, *et. al.*, *Phys. Plasmas* Vol. 9, No. 3 (2002).
- [3] S. Atzeni, A. Schiavi, and J. R. Davies, Plasma Phys. Control. Fusion 51 (2009) 015016

Field equations assume a resistive fluid background plasma

Zuma uses Ohm's law to determine E: $\vec{E} = \eta \vec{J}_b$

where J_b is the background current density. The resistivity is given by the Lee-More model for dense plasmas[1].

Substitute into Ampere's law, neglecting the displacement current (J_f is the fast electron current):

$$\vec{J} = \vec{J}_b + \vec{J}_f = \nabla \times \frac{B}{\mu}$$

$$\vec{E} = -\eta \vec{J}_f + \frac{\eta}{\mu} \nabla \times \vec{B}$$

$$\frac{\partial \vec{B}}{\partial t} = -\nabla \times \vec{E}$$

[1] Y. T. Lee and R. M. More, *Phys. Fluids* 27 (5) (1984)

Coordinate formulations of dψ/ds couples rays through directional advectors, reducing ray effects

cartesian

0

$$\frac{d\psi}{ds} \equiv \frac{dx}{ds}\frac{\partial\psi}{\partial x} + \frac{dy}{ds}\frac{\partial\psi}{\partial y} + \frac{dz}{ds}\frac{\partial\psi}{\partial z} + \frac{d\xi}{ds}\frac{\partial\psi}{\partial\xi} + \frac{d\varpi}{ds}\frac{\partial\psi}{\partial\varpi}$$

$$= \sqrt{1-\xi^2}\cos\varpi\,\frac{\partial\psi}{\partial x} + \sqrt{1-\xi^2}\sin\varpi\,\frac{\partial\psi}{\partial y} + \xi\,\frac{\partial\psi}{\partial z}$$

spherical

$$\frac{d\psi}{ds} \equiv \frac{dr}{ds}\frac{\partial\psi}{\partial r} + \frac{d\theta}{ds}\frac{\partial\psi}{\partial\theta} + \frac{d\vartheta}{ds}\frac{\partial\psi}{\partial\vartheta} + \frac{d\mu}{ds}\frac{\partial\psi}{\partial\mu} + \frac{d\omega}{ds}\frac{\partial\psi}{\partial\omega}$$

$$= \mu\frac{\partial\psi}{\partial r} + \frac{\sqrt{1-\mu^2}\cos\omega}{r}\frac{\partial\psi}{\partial\theta} + \frac{\sqrt{1-\mu^2}\sin\omega}{r\sin\theta}\frac{\partial\psi}{\partial\vartheta} + \frac{1-\mu^2}{r}\frac{\partial\psi}{\partial\mu} - \frac{\sqrt{1-\mu^2}\cot\theta\sin\omega}{r}\frac{\partial\psi}{\partial\omega}$$

directional advectors

Polar S_N maintains spherical symmetry in capsule implosion test problem

Density contours

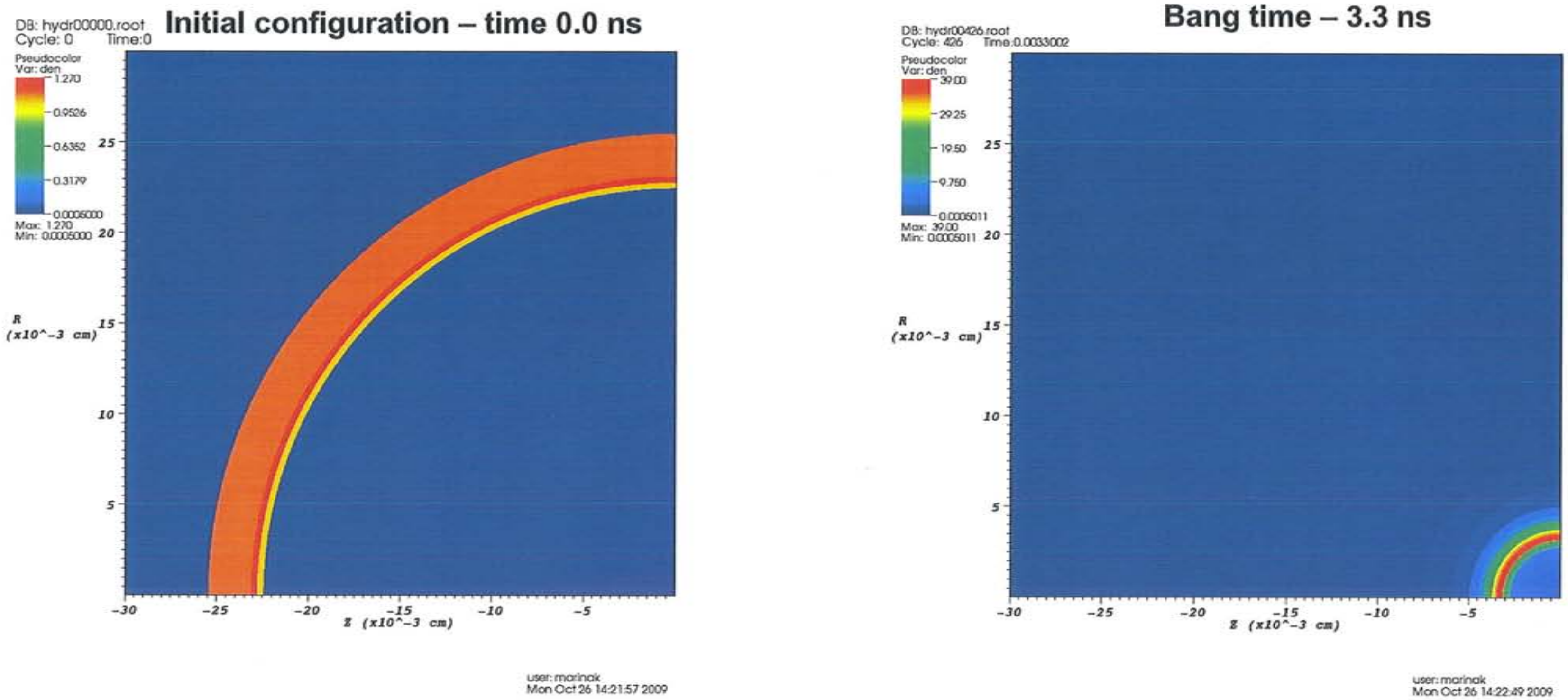

Simulation of Omega indirect drive capsule implosion
Uses 24 ray angles - 6 polar and 4 azimuthal

Radiation energy density agrees well with analytic solution throughout

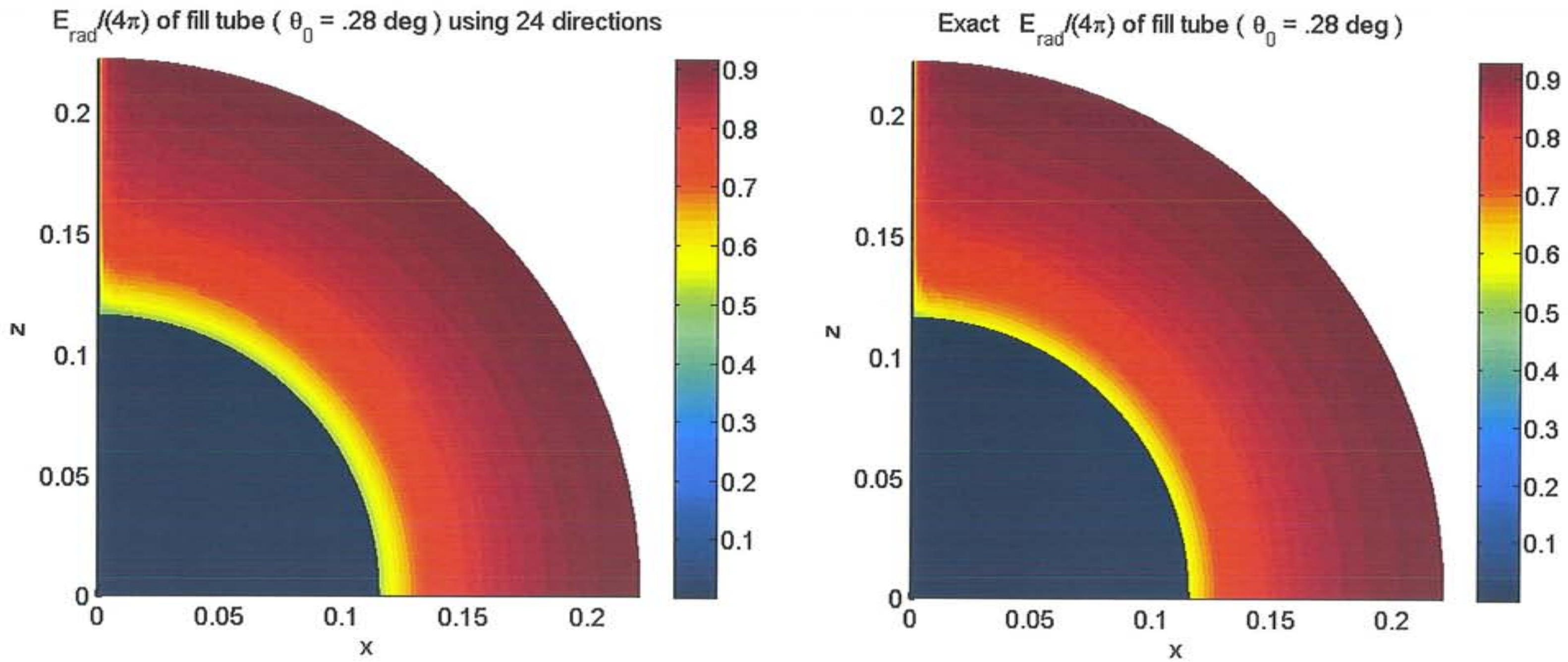

Burn profiles evolves toward axisymmetry despite non-uniform electron deposition profile

Material boundary 10 into pulse

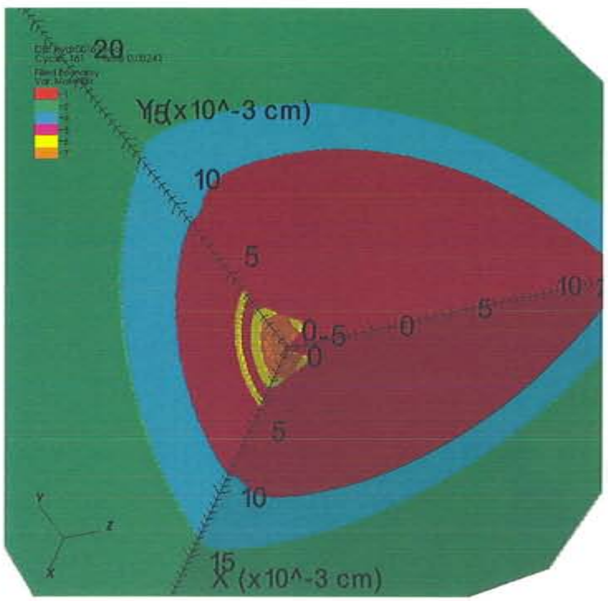

Density 10 psec into pulse (g/cm³)

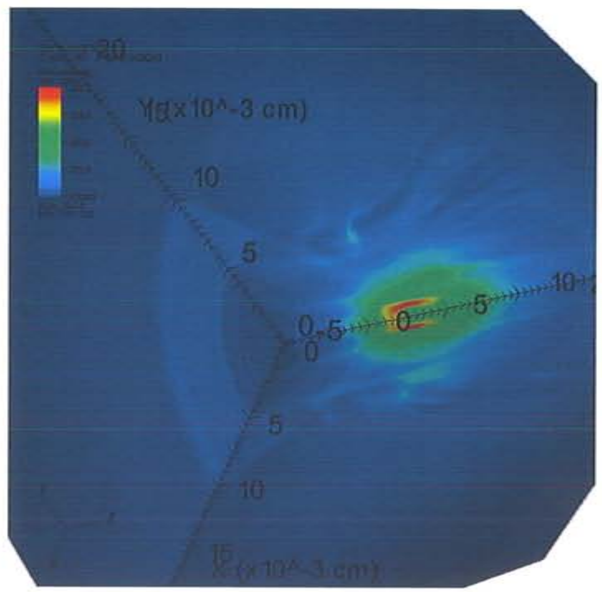

Ion temperature 20 psec after bang time

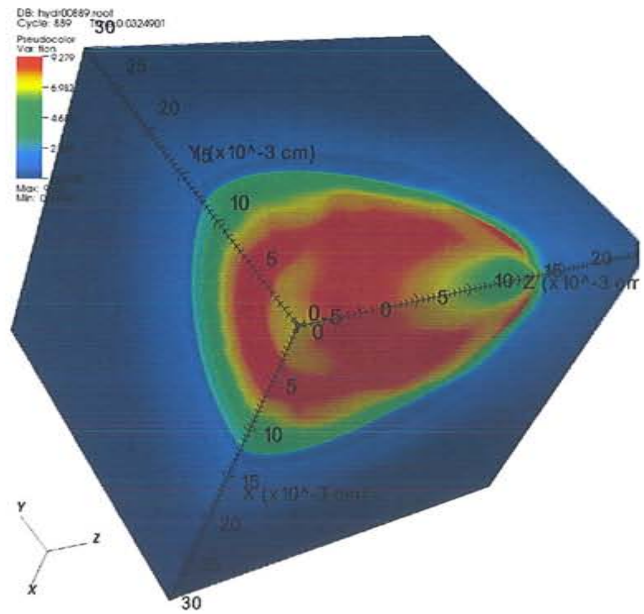

Capsule produces 3.74 MJ yield
Total electron energy 268.5 KJ, 125.2 KJ deposited in fuel
97.7 KJ electron energy lost

Cut planes at
x = 0, y = 0, z = -50 μm

$$\frac{\partial B}{\partial t} = \eta \nabla \times J_f + \nabla \eta \times J_f + \frac{\eta}{\mu} \nabla B - \frac{1}{\mu} \nabla \eta \times B$$